Magnetotransport in $Al_xGa_{x-1}As$ Quantum Wells with Different Potential Shapes

N. C. Mamani, C. A. Duarte, G. M. Gusev, A. A. Quivy, and T. E. Lamas
Instituto de Física da Universidade de São Paulo, CP 66318, CEP 05315-970, São Paulo, SP, Brazil

Received on 4 April, 2005

We compare the transport properties for triangular, parabolic and cubic quantum wells. We calculate the transport mobility for electrons belonging to the different subbands. We obtain the energy spacing between first and second subbands from the electron sheet density and compare results for different potential profiles. We find that experimental results are in quantitative agreements with our calculations.

Keywords: $Al_xGa_{x-1}As$; Transport properties; Quantum wells

I. INTRODUCTION

Recent progress in Molecular Beam Epitaxy (MBE) growth methods has made possible the creation of electronic systems with unusual and interesting properties. Well-known examples are double quantum wells, quantum dot array in different configurations and combination of layers and quantum dots [1–3]. MBE growth also can be used to grow quantum wells, when electrons are confined in potential with various profiles $U(z) = U_0|z/W|^n$, where W is the well-width parameter, U_0 is the potential height and n is number, which, is equal to 1 for triangular well and n=2 for parabolic well. Energy levels for these different potential wells have a different dependence on the quantum numbers. For example energy levels for the square well of infinite height are proportional to the square of the quantum number. For the parabolic well of infinite height the energy levels are evenly spaced. The energy levels for the potential $U(z) = U_0|z/W|^{2/3}$ exhibit a square-root dependence on the quantum number [4]. It is expected, that for low electron density in the well the "bare" potential is not screened and energy spectrum is not strongly modified. Since the many transport properties of electrons depend on the shape of the wave function and quantum well profile, it will be useful to identify the most suitable quantum well structure for new electronic devices development. In present paper we grew and studied $Al_xGa_{x-1}As$ quantum wells with potential shapes $U(z) = U_0|z/W|^n$, where n=1,2 and 3. For magnetic field oriented perpendicular to the sample a series of equidistant Landau levels are developed for the two-dimensional electron gas (2DEG), and magnetoresistance manifests Shubnikov -de Haas (SdH) oscillations. From analysis of the SdH oscillations we may deduce electron density for all electric subbands.

In present paper we grew triangular, parabolic and cubic $Ga_{1-c}Al_cAs$ quantum wells and compared its transport properties.

II. EXPERIMENTAL RESULTS AND DISCUSSIONS

The samples were made from $Ga_{1-c}Al_cAs$ quantum wells grown by molecular -beam epitaxy. It included a 2000 $\AA$ - wide $Ga_{1-c}Al_cAs$ wells with Al content varying between 0 and 0.21, bounded by undoped $Ga_{1-c}Al_cAs$ spacer layers with $\delta - Si$ doping on two sides [6]. The mobility of the electron gas in our samples was $\sim (100-350)\times 10^3 cm^2/Vs$ and density - $n_s = (2-4)\times 10^{11} cm^{-2}$, therefore our quantum wells were partially full with 1-4 subbands occupied. Four -terminal resistance R_{xx} and Hall R_{xy} measurements were made down to 1.5 K in a magnetic field up to 12 T. The characteristic bulk density for parabolic quantum well is given by equation $n_+ = \frac{\Omega_0^2 m^* \varepsilon}{4\pi e^2}$. The effective thickness of the electronic slab can be obtained from equation $W_{eff} = n_s/n_+$. For partially filled quantum well W_e is smaller than the geometrical width of the well W. We varied the electron sheet density by illumination with a red light-emitting diode.

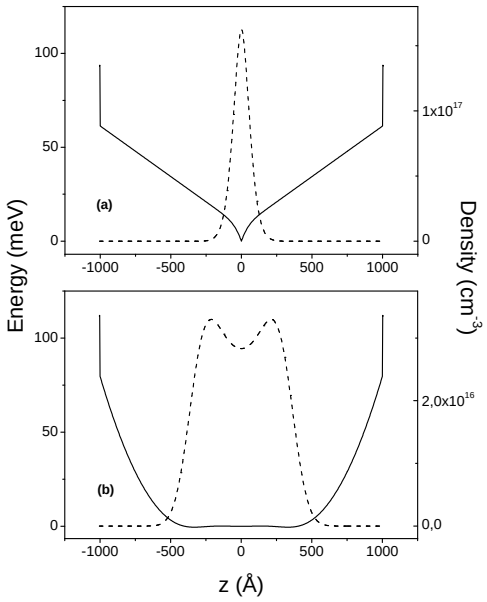

FIG. 1. Total potential (solid line) and electron density (dashes) as a function of position in the well for triangular (a) and parabolic quantum wells (b) before illuminations ($n_s = 2.4\times 10^{11} cm-2$).

Table 1. Comparison of the triangular and parabolic quantum wells for $n_s = 2.4\times 10^{11} cm^{-2}$. N is the number of occupied subbands.

Sample	N	$E_F - E_1$ meV	$E_F - E_2$ meV	$E_F - E_3$ meV	Δ $\AA$
parabolic	3	4.2	2.85	0.56	819
triangular	1	7.63	-	-	150

We performed full self-consistent calculations of the total potential, envelope wave functions, the eigenvalues energies and electron density in quantum wells with different shapes following a procedure similar to those used for parabolic quantum wells [5, 6]. Figs.1 and 2 show the electron density profile and total potential for triangular, parabolic and cubic quantum wells. We may see that the electronic slab width in parabolic quantum well is wider than in triangular well for the same carrier density. For cubic profile the quantum well is almost full for low electron density, therefore we are not able to do such comparison. The density profile depends on the number of substantially occupied subbands: when only one subband is occupied, the density profile is sharply peaked, as we see for triangular well. The table 1 summarize the results of the calculations of the Fermi level for different subbands in parabolic and triangular wells.

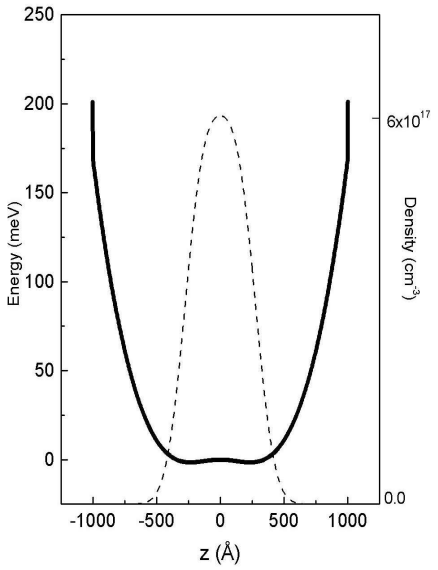

FIG. 2. Total potential (solid line) and electron density (dashes) as a function of position in the well for $U(z) = U_0|z/W|^3$ quantum well, $n_s = 0.6 \times 10^{11} cm^{-2}$.

We also calculate single particle relaxation time and transport relaxation time due to the background impurity doping. It is worth to note that the single particle relaxation time, or quantum time describes the decay time of one-particle excitations and give rise to the renormalization of the density of states in contrast to the transport relaxation time, which describes the mobility of an electron gas. The quantum times are obtained by numerical integration the squared matrix elements over the allowed scattering vector using self consistent calculated wave function. Screening of the impurity scattering potential in the presence of the 2D electron gas is included within the Thomas-Fermi approximation. A detailed calculation of the quantum and transport times should include the different scattering mechanism such as homogeneous background scattering, interface roughness scattering and alloy disorder scattering. The scattering time contains many parameters, such as concentration of the background impurities, which can be enhanced in parabolic well due to the greater reactivity of Al with oxygen, and roughness of the interfaces.

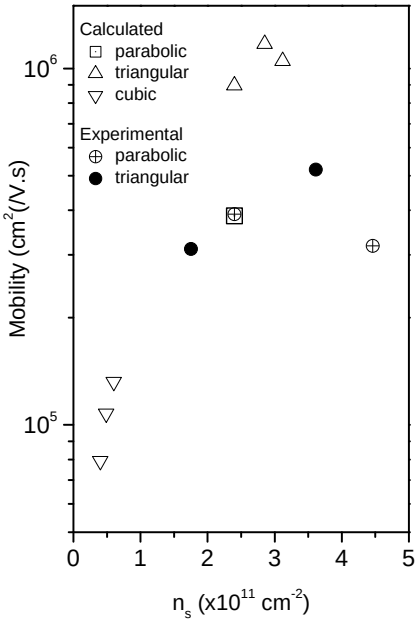

FIG. 3. The total mobility was calculated as a function electron density for parabolic, triangular and cubic wells. Solid circles-experimental results for triangular well, crossed circle-experimental mobility for parabolic well.

We do not attempt to calculate all scattering mechanisms accurately, because we are only interested its density profile behaviour. Since the wavefunction in our structures are located mostly in the center of the well we ignore the remote impurity scattering mechanism and suppose that the background impurities should be a major scattering mechanism in this case. It is worth to note that in the multi-subband systems the intersubband scattering starts to play very important role. For a system with N subbands occupied the quantum time is given by

$$1/\tau_q^i = \sum_{j=1}^{N} P_{ij}^0 . \qquad (1)$$

where P_{ij} is the transition rate for an incident electron in the i into j subband averaged over the allowed scattering vector. It is worth to note, that for the transport time equation (1) is not valid.

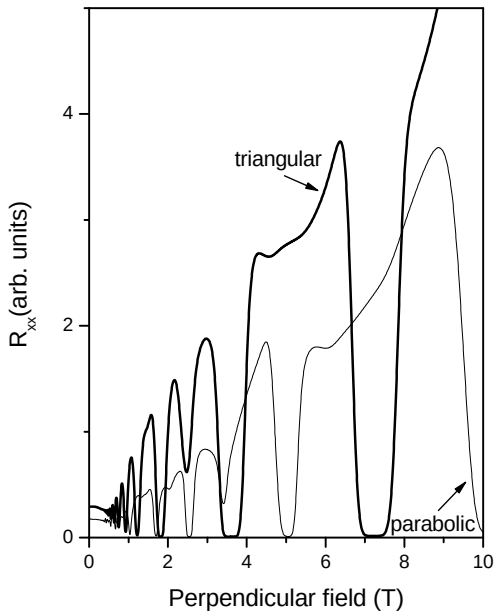

FIG. 4. Magnetoresistence as a function of the perpendicular magnetic field for parabolic (thin line) and triangular (thick line) quantum wells, T=1.5 K.

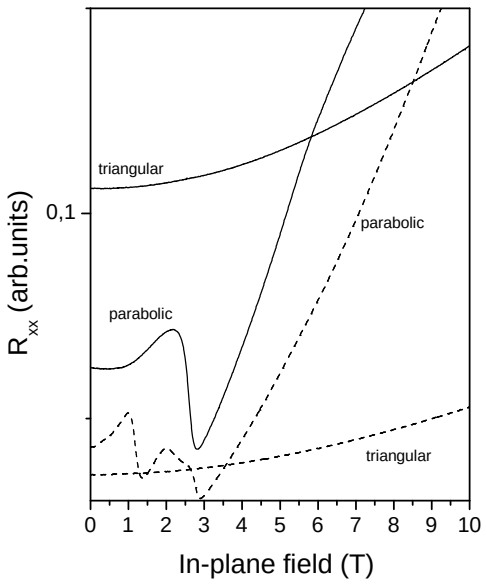

FIG. 5. Magnetoresistance as a function of the in-plane magnetic field for parabolic and triangular quantum wells, before illuminations (thick line) and after some short illumination by red diode (dashes), T=1.5 K.

The transport life time τ_{tr}^{i} has a more complicated form and can be obtained from the Boltzman equation [7]:

$$k_i \tau_{tr}^{i} = \sum_{j=1}^{N} (K_{ij})^{-1} k_j \,. \tag{2}$$

where the scattering matrix K_{ij} is defined as:

$$K_{ij} = \sum_{j=1}^{N} P_{ij}^{0} \delta_{ij} - P_{ij}^{1} \,. \tag{3}$$

The coefficient P_{ij}^{0} is the transition rate integrated over the allowed scattering vectors, and P_{ij}^{1} is the first component of the Fourier transform of this transition rate. The intersubband scattering terms appear both in the diagonal and off-diagonal matrix elements. However, our system is symmetrical and the intersubband scattering between subbands of different parities vanishes. We invert the matrix K_{ij} numerically, and obtain the transport life time for electrons in each subband. The effective average mobility is given by:

$$\mu = \sum_{j=1}^{N} \frac{n_i \mu_{tr}^{i}}{n_s} \,. \tag{4}$$

where $\mu_{tr}^{i} = (e/m)\tau_{tr}^{i}$. We fit the calculated mobility to the measured one for parabolic well and obtain background impurity concentration $N_{imp} = 1.2 \times 10^{14} cm^{-2}$.

The Fig. 3 shows the results of the transport relaxation times simulation for triangular, parabolic and cubic wells. The experimental transport time can be derived from the zero field mobility $\mu = e\tau_{tr}/m$. We may see that the mobility in triangular well is expected to be much higher than in parabolic well. We attribute it to the narrow density profile in triangular well. Note, however, that the experimental transport mobility in triangular well is less than the expected value. It is reasonable to assume that alloy disordered scattering is stronger in triangular well and can explain this difference. For cubic well we obtain low mobility, and more attempts to growth such samples are necessary. Fig. 4 shows high magnetic field magnetoresistance data for triangular and parabolic wells. We may see that for the same $\delta - Si$ doping, however, the parabolic well has larger electron density. From low field part of the SdH oscillations we deduce the electron density for each subbands and obtain results which are close to the calulated values (table.1). When 2DEG occupies several subbands, for magnetic field oriented in plane of the sample an additional type of magnetoresistance oscillations arises from the crossing of the diamagnetically shifted subband energies through the Fermi energy, the so-called diamagnetic Shubnikov-de Haas effect. Fig. 5 shows such oscillations for both profiles and for different electron densities. We may see that magnetoresistance for triangular well does not show any oscillations, since the electrons occupy only single subband, in contrast to the parabolic well, which shows 2-3 oscillations.

III. CONCLUSION

We report the comparison of the transport properties for triangular, parabolic and cubic quantum wells. We calculate the transport mobility for electrons belonging to the different subbands and find that triangular well has higher mobility. In the presence of an electric field the minimum of the confining potential may be displaced with the center of the well, whereas the implicitly of the envelope of the wave function is conserved. This particular property of the partially filled triangular well makes it suitable for the practical realization of the electronic devices based on the manipulation of the g-factor for spintronic application[8].

Acknowledgments

Support of this work by FAPESP, CNPq (Brazilian agencies) is acknowledged.

[1] J. P. Eisenstein, L. N. Pfiefer, and K. W. West, Phys. Rev. Lett. **69**, 3804 (1992).
[2] A. P. Alivisatos, Science, **271**, 933 (1999).
[3] A. S. G. Thornton, T. Ihn, P. C. Main, L. Eaves, K. A. Benedict, and M. Henini, Physica B **249-251**, 689 (1998).
[4] S. K. Sputz, A. C. Gossard, Phys. Rev. B **38**, 3553 (1988).
[5] A. J. Rimberg, R. M. Westervelt, Phys. Rev. B **40**, 3970 (1989).
[6] C. S. Sergio, G. M. Gusev, J. R. Leite, E. B. Olshanetskii, N. T. Moshegov, A. K. Bakarov, and A. I. Toropov, D. K. Mau-de, O. Estibals, and J. C. Portal, Phys. Rev. B **64**, 115314 (2001).
[7] E. Zaremba, Phys. Rev. B **45**, 14143 (1992).
[8] G. Salis, Y. Kato, K. Ensslin, D. C. Driscoll, A. C. Gossard, and D. D. Awschalom, Nature **414**, 619 (2001).